

SUPPLEMENTARY TEXT:PTEN Cleft Binding Site Mutations:

In order to investigate PIP₃ binding to the PTEN cleft between the C2 domain and PD, 4 residues on PTEN (K164, K269, K327 and K330) were mutated from lysine to glutamic acid in order to change the charge distribution of the PTEN cleft (Supporting Information Fig. S1). Simulations were then run for 1 μ s using the set up described in the main text using a bilayer with 1 PIP₃ in the PTEN bound leaflet (see Fig. 3). No binding of PIP₃ to the PD/C2 cleft site was observed in any of the simulations, in contrast to the results obtained using the wild type PTEN. This suggests that the charge reversal of the mutated residues and the reduction of electrostatic interaction inhibited the binding of PIP₃ lipids to the previously observed cleft binding site. The PIP₃ lipids did not bind to any alternative conserved site. Similar to the wild type simulations the PD domain formed transient interactions with the bilayer.

Interaction of PTEN with bilayers containing both PIP₂ and PIP₃:

After studying the association of PTEN with PIP₃-containing bilayers, CG-MD simulations investigating the binding of PIP₂ to PTEN were carried out using the systems described in Table S1. Similar simulations to those described in Fig. 3 of the main text were run with one or four PIP₂ lipids in a POPC/POPS bilayer. PTEN interacted with the bilayer with the C2 domain in all cases. However the PD domain interacted with the bilayer only when the PIP₂ molecule bound to the PD. Thus, PIP lipids appear to act as a ‘PD anchor’ (via residues R15 and R161 in one case, and Y16 and T160 in the other). As well as interacting with the C2 domain and PD, PIP₂ molecules also interacted with the cleft between the two domains at residue K330 in two of the simulations with four PIP₂ in the bilayer.

As both PIP₂ and PIP₃ had been shown to interact with the cleft between the PD and the C2 domain, CG-MD simulations were run with a bilayer containing both 4 PIP₂ molecules and 4 PIP₃ molecules (*pten_bound-6*). This was done in order to determine if the two different types of PIP molecules would compete for binding to the PTEN cleft site between the C2 domain and PD. The results showed an almost equal chance for either PIP species to bind to the cleft site. Two out of six simulations showed PIP₃ binding and three out of six showed PIP₂ binding to the cleft (the remaining simulation showed no binding). The orientation of PTEN to the bilayer was as described above.

Interaction of PTEN with PIP₂-containing bilayers:

To determine whether the presence of PIP₂ molecules in the bilayer will affect the mechanism of PTEN association with the bilayer, simulations with the PTEN displaced 9 nm away from a POPC:POPS:PIP₂ (75:20:5) lipid bilayer were also performed. In all simulations PTEN initially diffuses in the aqueous environment before forming a complex with the bilayer. Similar to the simulations with the PIP₃-containing bilayers the initial encounter of PTEN is followed by reorientation of PTEN on the bilayer surface to form more specific interactions with the lipids in the bilayers. When PTEN reaches its final productive orientation (see main text for the definition of the productive orientation) then this orientation is retained for the remainder of the simulation. In the productive orientation, which is the same as in the simulations with the PIP₃-containing bilayers, the C2 domain associates with the bilayer with the same positively charged region as identified above (region 1 in Supplementary Figure S1). PD initially forms transient interactions with the

bilayer but these interactions are stabilized after its association with PIP₂ lipids in the bilayer. Lysine and arginine residues form the largest number of contacts and are the same as those described for the simulations of the PTEN with PIP₃-containing bilayers. Additionally, after PTEN adopts its final productive orientation relative to the bilayer, clustering of PIP₂ molecules around the protein occurs. All the results for the *pten_away-pip2* simulation are shown in Supplementary Figure S9.

Table S1: Summary of the additional simulation with PTEN

| Simulation | Bilayer composition | Number of PIPs | Duration (ns) |
|-----------------------|--------------------------------------|---|---------------|
| <i>pten_bound-4</i> | POPC:POPS (80:20) | 1 PIP ₂ in PTEN bound leaflet | 7 x 1 μs |
| <i>pten_bound-5</i> | POPC:POPS (80:20) | 4 PIP ₂ in PTEN bound leaflet | 6 x 1 μs |
| <i>pten_bound-6</i> | POPC:POPS (80:20) | 4 PIP ₂ and 4 PIP ₃ in PTEN bound leaflet | 6 x 1 μs |
| <i>pten_away-pip2</i> | POPC:POPS:PIP ₂ (75:20:5) | | 6 x 3 μs |

SUPPLEMENTARY FIGURES:

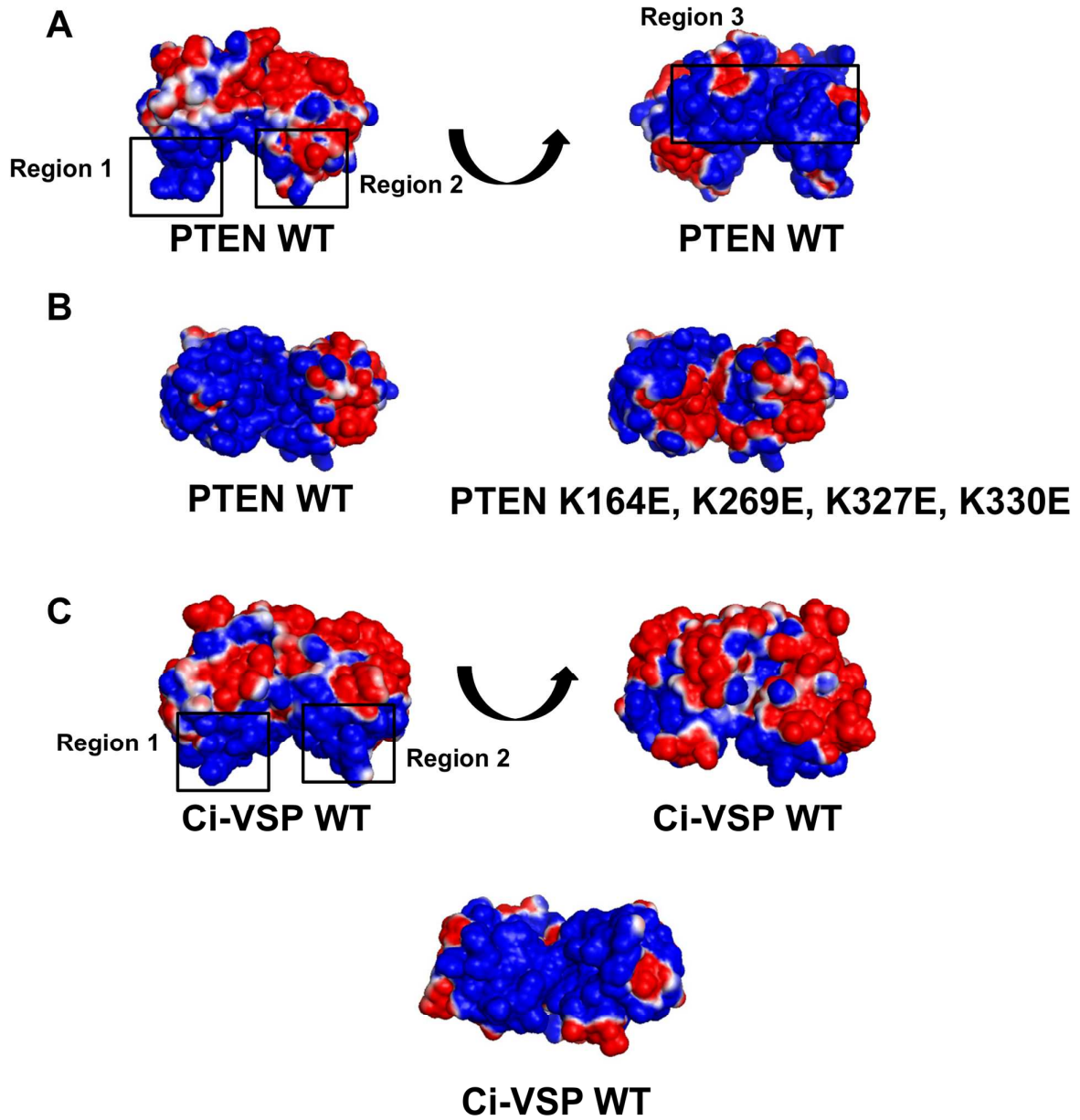


Figure S1:

Electrostatic surface of PTEN for the wild type (A) and the mutant form (B). The same analysis is shown for the wild type Ci-VSP (C). Blue indicates a positive surface and red a negative surface. The electrostatic calculation was performed using APBS ⁽¹⁾ in PyMol ⁽²⁾. The electrostatic potential ranges from -1.5kT/e (red) to +1.5kT/e (blue).

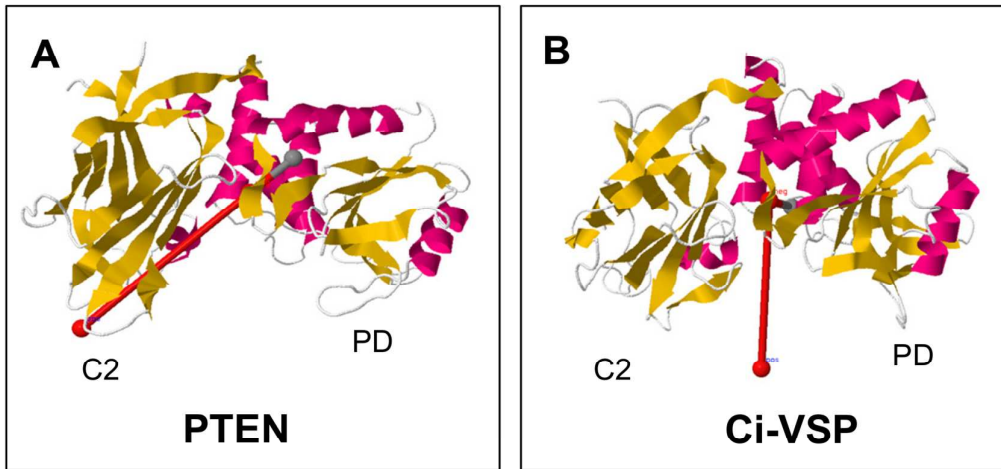


Figure S2:

A,B. Dipole moment for the PTEN (A) and the Ci-VSP (B). The dipole moment was calculated using an online server (<http://dipole.weizmann.ac.il>).

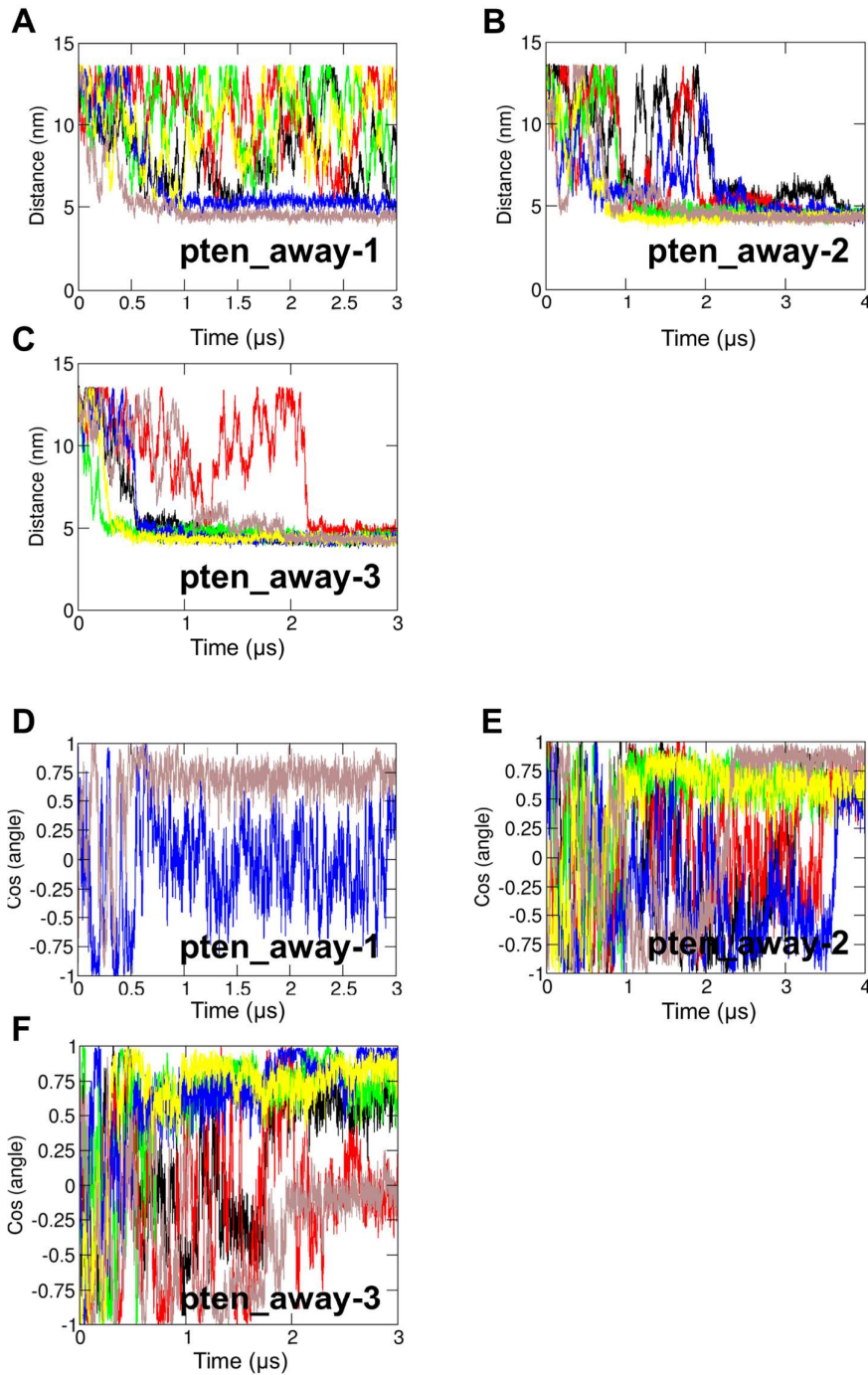


Figure S3:

A,B,C. Progress of the simulations with the PTEN and PIP₃-containing bilayers (*pten_away-1* to -3 simulations in Table 1). The progress of the simulations is shown as the separation between the centres of mass of the protein and the bilayer as a function of time. The six different colours represent the six different repeat simulations performed for each system. D,E,F. The cosine of the angle between the plane of the protein and the bilayer plane is shown for the individual simulations as a function of time (shown using the same colour coding as in A, B, C). The cosine is shown only for simulations which resulted in a PTEN/bilayer complex for clarity.

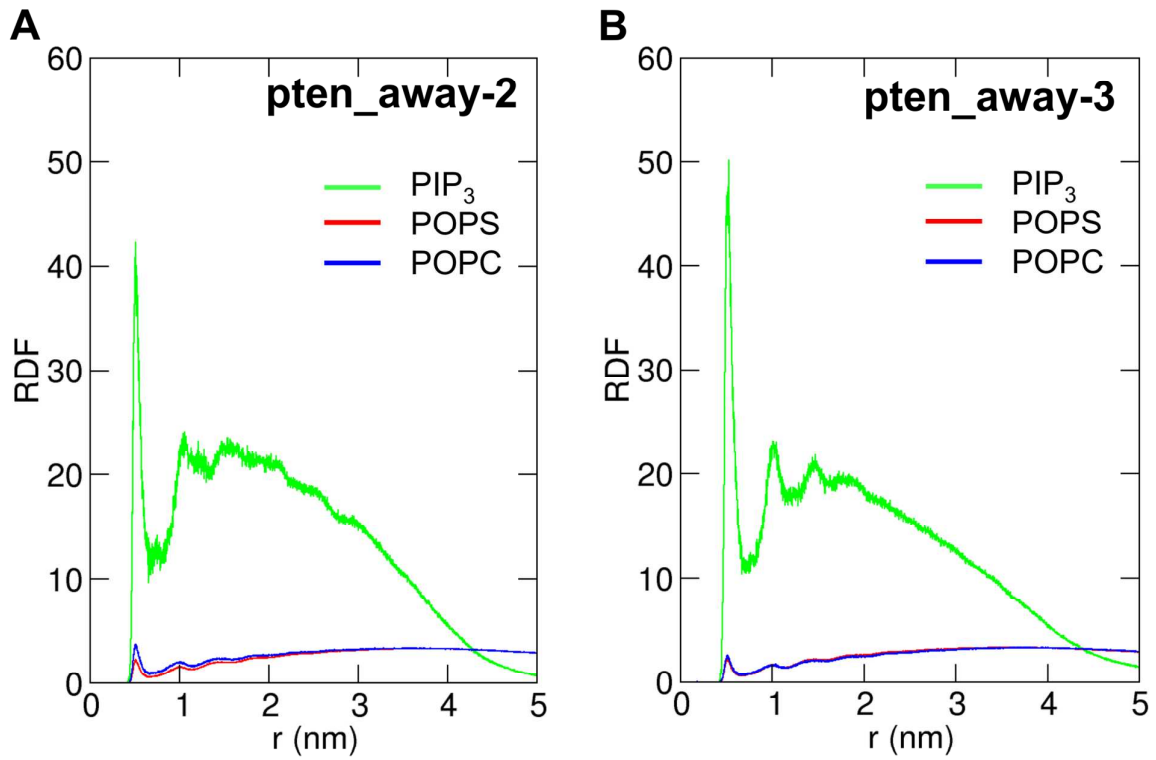


Figure S4:

A,B. The lipid radial distribution function for the *pten_away-2* (A) and the *pten_away-3* simulations (B). The distribution for each lipid type (i.e. POPC, POPS and PIP_3 lipids) is an average over all the repeat simulations which resulted in a PTEN/bilayer complex. The radial distributions were calculated around the PTEN domain.

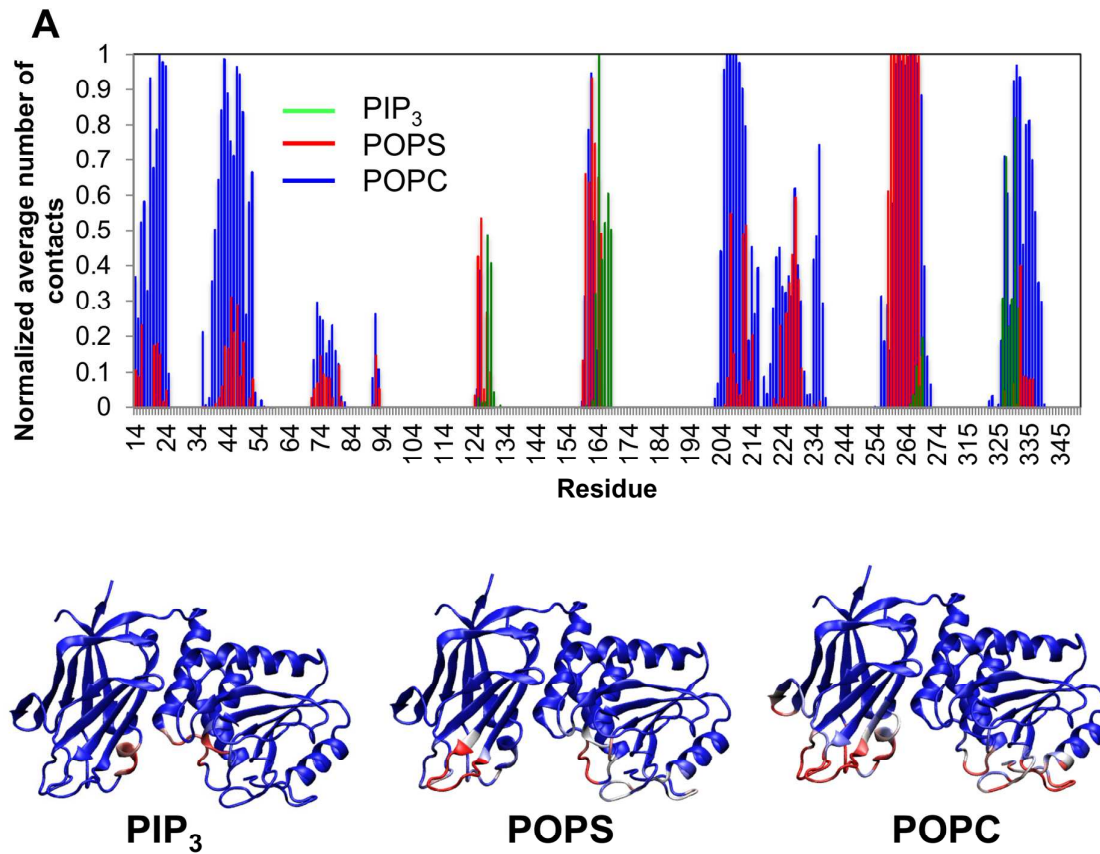


Figure S5:

A. Normalized average number of contacts (using a cut-off distance of 3.5 Å) between the PTEN and the lipids in the bilayer (across all repeats of the AT-MD simulations with the PIP₃/POPC/POPS bilayer; simulation *pten_AT-1* in Table 1). The normalized average number of contacts for each lipid type was mapped on the PTEN crystal structure. Blue indicates a low number, white indicates a medium number and red a large number of contacts.

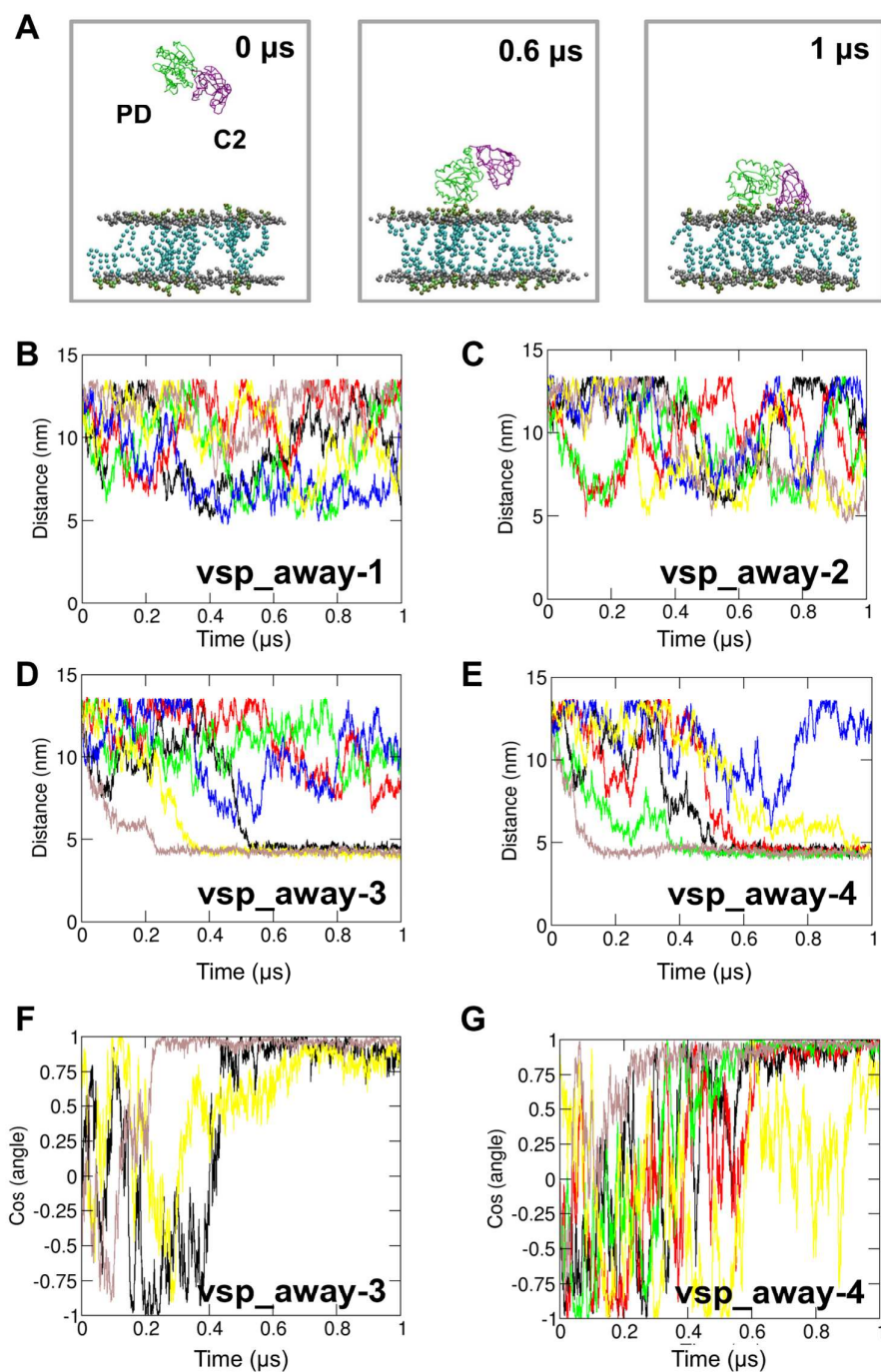
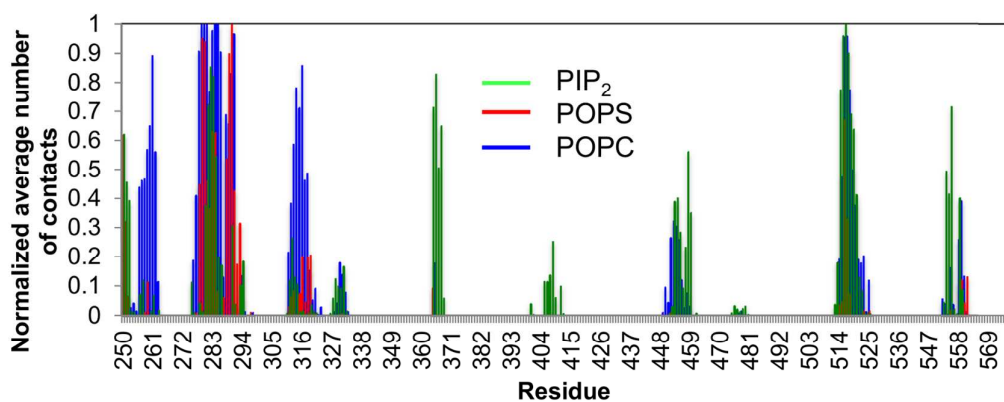


Figure S6:

A. Progress of the simulations with the Ci-VSP. Snapshots are shown from the *vsp_away-3* system at 0 μs , 0.6 μs and 1 μs . The Ci-VSP PD is shown in green and the C2 domain in purple. The POPC and POPS headgroups are shown as grey spheres and the PIP₂ lipids are shown in VDW format. B,C,D,E. Separation between the centers of mass of Ci-VSP and the bilayer as a function of time for the simulation with the wild type Ci-VSP and different bilayers (simulations *vsp_away-1* to 4 in Table 2). The six different colours represent the six different repeat simulations performed. F,G. The cosine of the angle between the plane of the protein and the bilayer plane is shown for the systems with PIP₂ and PIP₃ lipids as a function of time for the simulations that yielded a Ci-VSP/bilayer complex (shown using the same colour coding as in D and E).

A



B

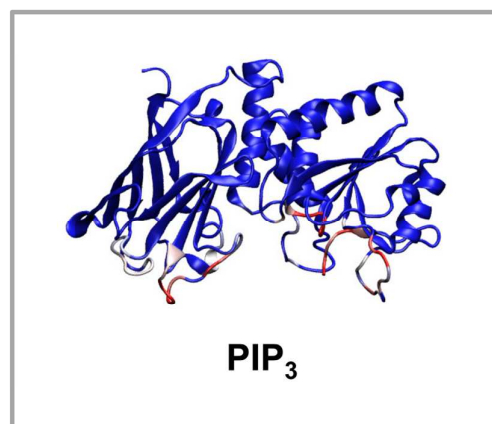
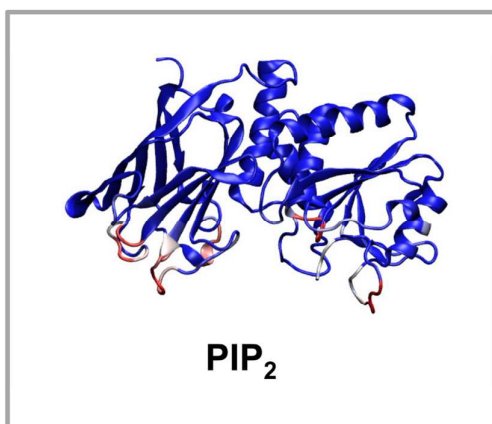
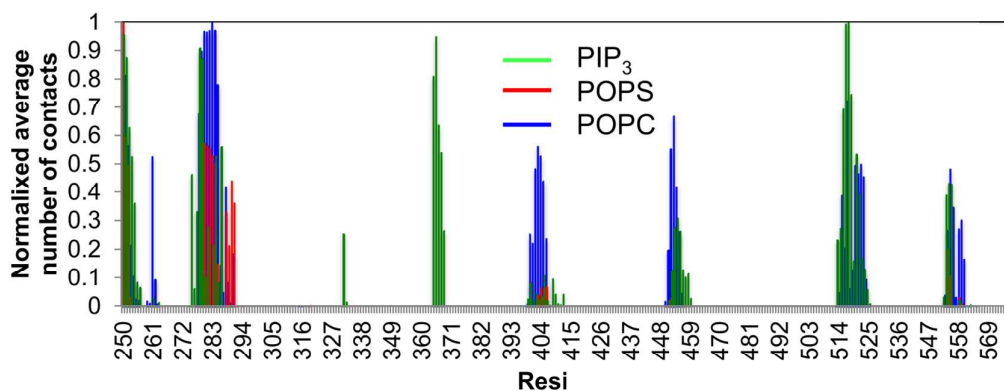


Figure S7:

A. Normalized average number of contacts (using a cut-off distance of 3.5 Å) between the Ci-VSP and the lipids in the bilayer (across all repeats of the *vsp_AT-1* and *vsp_AT-2* simulations in Table 2). The normalized average number of contacts for PIP lipids in each system was mapped on the Ci-VSP structure. Blue indicates a low number, white indicates a medium number and red a large number of contacts.

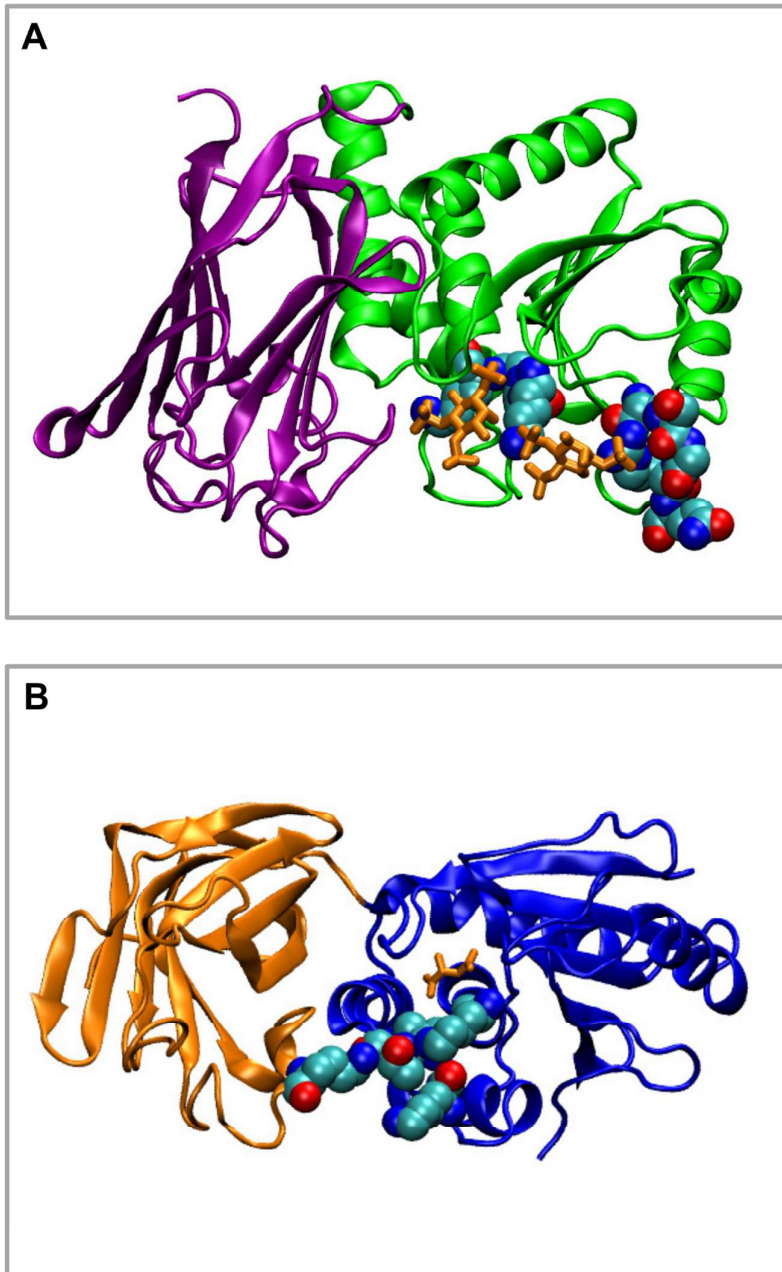


Figure S8:

A,B. The residues that we identified from our simulations to make the largest number of contacts with the PIP₂ or PIP₃ lipids are shown on the Ci-VSP (A) and the PTEN (B) crystal structures. The tartrates from the crystal structures are shown in orange.

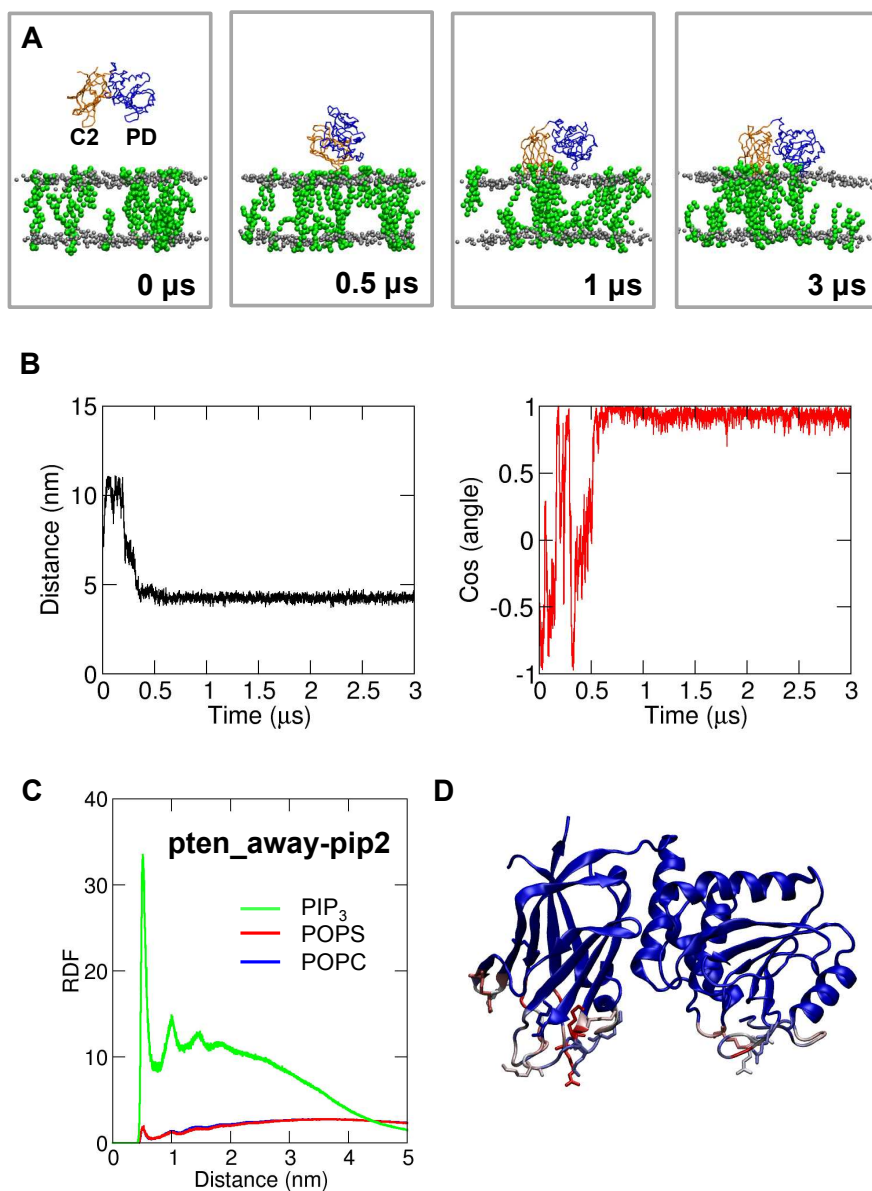


Figure S9:

A. Progress of a selected simulation (*pten_away-pip2* in Table S1) with the PTEN molecule displaced away from a bilayer that contained 5% PIP₂ molecules (green) in each leaflet. Simulation snapshots are shown at 0 μ s, 0.5 μ s, 1 μ s and 3 μ s. PTEN C2 domains and PD are colored as above.

B. Distance between the centre of mass of the protein and the centre of mass of the bilayer (left) and the cosine of the angle made between the protein plane and the bilayer plane (right) as a function of time for the simulation in A. This angle is equal to 0° (and hence the cosine is equal to 1) if the protein is in the 'correct' binding orientation (see text for more information).

C. The mean lipid radial distribution function for the *pten_away-pip2* simulation. The distribution for each lipid type (i.e. POPC, POPS and PIP₃ lipids) is an average over all the repeat simulations. The radial distributions were calculated around the PTEN domain.

D. Normalized average number of contacts (using a cut-off distance of 0.7 nm) between the PTEN and the lipids in the bilayer (across all repeats of the *pten_away-pip2* simulation in Table S1). The normalized average number of contacts was mapped on the PTEN structure. Blue indicates a low number, white indicates a medium number and red a large number of contacts. All lysine and arginine residues on the protein/bilayer interface are also shown.

REFERENCES:

1. Baker, N. A., Sept, D., Joseph, S., Holst, M. J., and McCammon, J. A. (2001) Electrostatics of nanosystems: application to microtubules and the ribosome, *Proc. Nat. Acad. Sci. USA* 98, 10037-10041.
2. DeLano, W. L. (2002) The PyMOL Molecular Graphics System, <http://www.pymol.org>.